Ultrafast Ge-Te bond dynamics in a phase-change superlattice

Marco Malvestuto,[1,*] Antonio Caretta,[1] Barbara Casarin,[1,2] Federico Cilento,[1] Martina Dell'Angela,[1] Daniele Fausti,[2] Raffaella Calarco,[3] Bart J. Kooi,[4] Enrico Varesi,[5] John Robertson,[6] and Fulvio Parmigiani[1,2,7]

[1]*Elettra-Sincrotrone Trieste S.C.p.A. Strada Statale 14 - km 163.5 in AREA Science Park 34149 Basovizza, Trieste, Italy*
[2]*Department of Physics, University of Trieste, Via A. Valerio 2, 34127 Trieste, Italy*
[3]*Paul-Drude-Institut für Festkörperelektronik, Hausvogteiplatz 5-7, 10117 Berlin, Germany*
[4]*Zernike Institute for Advanced Materials, University of Groningen, Groningen 9747 AG, The Netherlands*
[5]*Micron Semiconductor Italia S.r.l., Via C. Olivetti, 2, 20864 Agrate Brianza, MB, Italy*
[6]*Engineering Department, Cambridge University, Cambridge CB2 1PZ, United Kingdom*
[7]*International Faculty, University of Cologne, 50937 Cologne, Germany*
(Received 26 May 2016; revised manuscript received 28 July 2016; published 29 September 2016)

A long-standing question for avant-garde data storage technology concerns the nature of the ultrafast photoinduced phase transformations in the wide class of chalcogenide phase-change materials (PCMs). Overall, a comprehensive understanding of the microstructural evolution and the relevant kinetics mechanisms accompanying the out-of-equilibrium phases is still missing. Here, after overheating a phase-change chalcogenide superlattice by an ultrafast laser pulse, we indirectly track the lattice relaxation by time resolved x-ray absorption spectroscopy (tr-XAS) with a sub-ns time resolution. The approach to the tr-XAS experimental results reported in this work provides an atomistic insight of the mechanism that takes place during the cooling process; meanwhile a first-principles model mimicking the microscopic distortions accounts for a straightforward representation of the observed dynamics. Finally, we envisage that our approach can be applied in future studies addressing the role of dynamical structural strain in PCMs.

I. INTRODUCTION

In these last years innovative fields for cutting-edge technologies based on novel engineered materials have been disclosed by the understanding of the nonequilibrium optical control of the matter.

For instance the comprehension of the nonequilibrium mechanisms is of paramount importance for exploiting the physical and optical properties of the phase-change materials (PCMs), nowadays used in optical data storage [1] and nonvolatile electrical memories [2].

The key feature of these intriguing compounds is the large and steep change of the optical and electrical properties observed when comparing the covalent bonded amorphous phase with the resonantly bonded crystalline phase. Interestingly, this scenario has been recently enriched by the GeSbTe chalcogenide (GST) superlattices (CSLs), that are regarded as novel phase-change materials [3,4], where the phase transition is between two crystalline structures, rather than amorphous to crystalline or vice-versa.

However, it is stimulating the fact that all these materials share common phase change properties, such as the switching time, the activation energy, and the dielectric response, hence suggesting that a similar physics must govern the complex nature of their local atomic structure and configuration conditions.

To shed light on these compelling mechanisms, some models, based mainly on thermal or electronic processes, have been proposed [5–16].

Conversely, other studies [17–22] suggest that more complex mechanisms are governing the atomic dynamics at the base of the phase switching, where concomitant thermal and electronic aspects compete in a synergic feedback loop [17]. Yet, the structural dynamics during fast temperature quenching processes of overheated GST glasses and crystals is still unclear [8,9]. Indeed, when the heating-cooling cycle between two structural phases is closely observed, a variety of parameters (from quenching velocity to thermal dissipation and/or structural strain) [23] dictate the out-of-equilibrium dynamical evolution in the energy phase space across either the amorphous-crystal or the crystalline-crystalline phase transformation [24]. Henceforth, the role of the quenching processes on the final structural configuration may not simply be a thermal dissipation, especially when the cooling rates are in the range of 10^{12} K/s or the heating stimulus is intense and ultrafast, i.e., in the ps time range. These considerations indicate that a comprehensive knowledge of the cooling phase in GSTs is paramount.

The scope of this work is thus to assess the role of the ultrafast thermal strain dynamics in a CSL structure during the first instants of the heating-cooling cycle. To this end, we cyclically heat a CSL sample slightly below its phase change temperature and observe the cooling phase by means of time-resolved x-ray absorption spectroscopy (tr-XAS) of the Ge L_3 edge. By mean of first-principles multiple scattering simulations for interpreting tr-XAS experiments, we unveil the microscopic structural and the dynamical changes occurring after the ultrafast heating of a nominal [GeTe(1 nm)/Sb_2Te_3(3 nm)]$_{15}$ CSL. The present results allow us to unambiguously ascribe the distinct features of tr-XAS spectra to the dynamical structural strain occurring during the thermal quenching process.

Recently, Ge L_3-edge XAS of GeTe based alloys [25,26] have been interpreted using real-space *ab-initio* multiple scattering simulations on crystalline and amorphous models. These

*marco.malvestuto@elettra.eu

and previous [27] studies have confirmed the effectiveness of the Ge L_3 edge as a spectroscopic probe to distinguish changes of the local atomic and electron charge distribution around the Ge photoabsorber. Therefore, by extending the Ge L_3 absorption edge measurement to the time domain, details about the local atomic structural dynamics during out-of-equilibrium states, like premelting phases and fast cooling processes, could be accessed. In addition, unlike x-ray diffraction, tr-XAS can be applied to both the crystalline and amorphous phases providing information about the projected density of states (pDOS).

II. EXPERIMENT

In the present experiment we probe an as-grown [GeTe(1 nm)/Sb$_2$Te$_3$(3 nm)]$_{15}$CSL, which has been grown on the Sb-passivated surfaces of Si(111), $(\sqrt{3} \times \sqrt{3})$R30∘-Sb, at a substrate temperature of 230 °C, and capped with a terminal layer for preventing oxidation [28,29]. The experiments have been carried out at the beamline BACH of the Elettra Synchrotron light source in Trieste, Italy, which operates an optical pump and x-ray probe technique capable of performing tr-XAS experiments with sub-ns time resolution, hence making possible the direct observation of the structural evolution on ultrafast time scales. A general description of the setup is reported elsewhere [30]. In its standard multibunch operating mode, the Elettra storage ring delivers x-ray pulses with (i) low intensity ($\sim 10^3$ photons/pulse in a quasimonochromatic beam), (ii) high repetition rate (500 MHz), and (iii) a ~ 100 ps full-width-at-half-maximum (FWHM) photon pulse temporal profile. This last parameter dictates the maximum time resolution of this experimental scheme. A Ti-sapphire amplified laser source operating at a ~ 233 kHz repetition rate and synchronized with the storage ring radio frequency is used and delivers pump pulses of up to 50 fs at 800 nm, with an energy/pulse of ~ 6 μJ. The time jitter of the laser with respect to the x-ray pulses is less then 5 ps, while the other relevant laser parameters are reported in Table I. The absorbed energy per pulse is calculated by measuring the sample transmittance response [31] in the 0.1–1 eV energy range and extrapolating the response function value at 1.55 eV (see discussion in Supplemental Material [32], paragraph I).

A simplified sketch of the experimental pump-probe configuration is represented in panel (a) of Fig. 1. The laser is focused on the sample by a 300-mm focal-length lens. Spatial overlap between x-ray and laser pulses is ensured by the alignment of both pump and probe beams using a 100 μm pinhole [30].

The time resolved XAS Ge L_3 edge was probed in fluorescence mode using an Hamamatsu ultrafast μ-channel plate [30] and acquired as a function of laser pulse time delay δt. The temporal overlapping of the pump and probe pulses defines the zero time delay ($\delta t = 0$). The dynamics is measured

TABLE I. Laser parameters.

Average power	400	mW
Wavelength λ	800	nm
Spot size	250	μm
Absorbed energy/pulse	0.75	μJ see Supplemental Material Ref. [32]
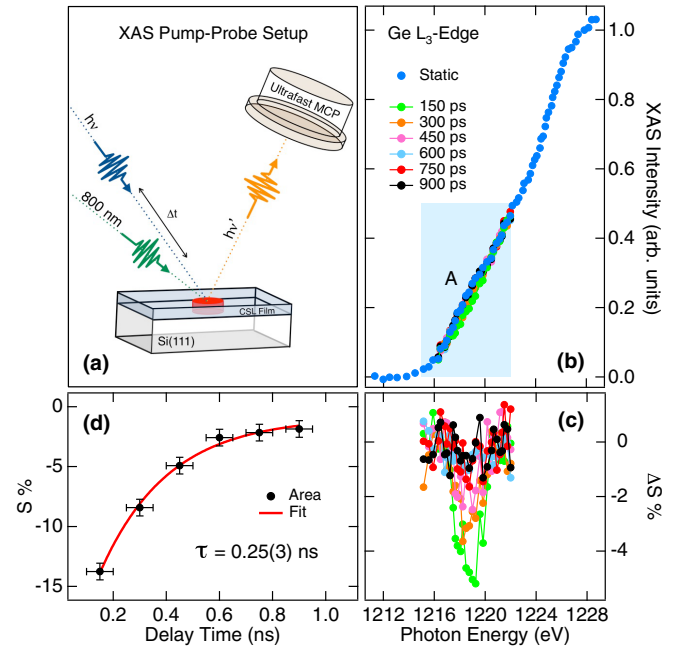
FIG. 1. Panel (a) reports a simplified sketch of the setup: the 800 nm laser beam and the synchrotron x-ray pulses, synchronized with delay Δt, are both impinging on a CSL film grown on a Si substrate. Panel (b) shows a collection of Ge L_3 edges taken at different time delays with time step $\delta t \sim 150$ ps, in comparison with a static Ge L_3 line shape (dotted blue curve). Panel (c) shows a close-up of the shoulder A in the $\Delta E = 1215$ to 1220 eV photon energy range [blue rectangle in panel (b)] plotted as $\Delta S(t)$ (see text). Panel (d) shows temporal dynamics of the spectral weight $S(t)$ (black dots; see text) fitted with a single exponential function.

in 150 ps time delay steps from $t = -150$ ps to $t = 900$ ps for an overall time interval Δt of ~ 1 ns.

III. RESULTS AND DISCUSSION

Figure 1(b) reports a near edge region of the Ge L_3-edge line shape (blue dotted curve) measured across the $2p_{3/2}$-sp absorption transition (~ 1220 eV).

The onset of the absorption edge is reported at equilibrium, i.e., without shining laser light on the sample, and after the preedge background removal and postedge normalization.

A tiny spectral bump A appears at the onset of the absorption threshold in the low energy region [blue box in Fig. 1(b)] being a direct signature of the specific local atomic Ge-Te coordination and electron charge distribution [26]. The measured photon energy range is limited to about 15 eV around the absorption threshold. In fact, as already reported elsewhere [26] and shown in this work by our calculations, the Ge sp hybridized states, which are responsible for the Ge-Te bonding, are projected over few eVs above the Fermi energy.

Upon laser illumination ($\delta t > 0$), a sudden ($\ll 150$ ps) but small change of the spectral weight of A is observed. Possible sample damaging has been monitored as a function of the laser fluence by acquiring consecutive static Ge L_3 edges and checking for possible changes of the line shape. The laser fluence used in our work was, in any case, far below the fluences used in previous works [15,16,33,34].

A collection of representative snapshots of the time evolution of the Ge L_3 edge as a function of time delay after the laser excitation is shown superimposed to the equilibrium threshold.

Magnified threshold changes over the bump energy region and time delays are displayed in Figs. 1(c) and 1(d), respectively, where the relative spectral weight change $\Delta S(E)$ [Fig. 1(c)] and the integrated threshold change $S(t)$ [Fig. 1(d)] are reported. $\Delta S(E)$ is calculated as the normalized difference between the threshold intensities as a function of δt and of the reference static L_3 edge:

$$\Delta S(E,\delta t) = \frac{S(E,\delta t = 0) - S(E,\delta t)}{S(E,\delta t = 0)}. \qquad (1)$$

$S(t)$ is then calculated by integrating $\Delta S(E)$ over the corresponding energy range:

$$S(t) = \int_{E1}^{E2} \Delta S(E,\delta t)\Delta E. \qquad (2)$$

It can be clearly seen that following the arrival of the laser pump pulse, $\Delta S(E)$ decreases and it reaches its minimum value after the first time delay step of ~150 ps. In addition, considering the temporal evolution of $S(t)$, the initial decrease is followed by its almost complete recovery in about 1 ns.

Since the overall time resolution is limited to the delay step that is comparable with the probe intrinsic time resolution (~ 100 ps), spectral changes at shorter delays cannot be appreciated. Hence, the laser excitation and the resulting heating process are too fast to observe.

Ge-L_3 XAS corresponding to either longer or negative time delays confirm that the L_3 shoulder remains unchanged and the measurement is reproducible. This important observation indicates that the material completely recovered the initial state and the impulsive heating-fast-cooling cycle is thus reversible.

For the sake of clarity, in the following part of the discussion we will assume that the probed volume of the sample has an average uniform temperature depending on δt. Thus temperature inhomogeneities, resulting from the depth dependent heat distribution due to the Beer-Lambert law of light absorption, are neglected. This assumption is validated by considering that the x-ray probe penetration depth at 1.2 KeV is ~ 800 nm [35]. Thus the XAS is providing an averaged information about the local structure. In addition, since the thermal heat dissipation of CSL is relatively high, heat flow smears out the temperature distribution within the probed volume in a few ps. It is worth to mention that the CSL/Si interface thermal resistance, which dictates the thermal flow from the CSL film through the bulk Si reservoir, is comparatively higher than the CSL thermal resistance.

The $S(t)$ temporal decay provides information on the dynamics, being $S(t)$ related to both the thermal dissipation and the structural relaxation. Accordingly, by using a one temperature model, the $S(t)$ was fitted with a single exponential function $a\exp^{-\frac{t}{\tau_0}}$, where τ_0 is found to be ~255 ps. The structure then relaxes with a cooling rate of 10^{12} K/s, which is comparable to that expected for similar glass forming systems [36–38].

Even more interesting is to investigate the role of crystalline structure on the observed spectral changes. Thus, we have computed multiple scattering (MS) simulations [39,40] of the
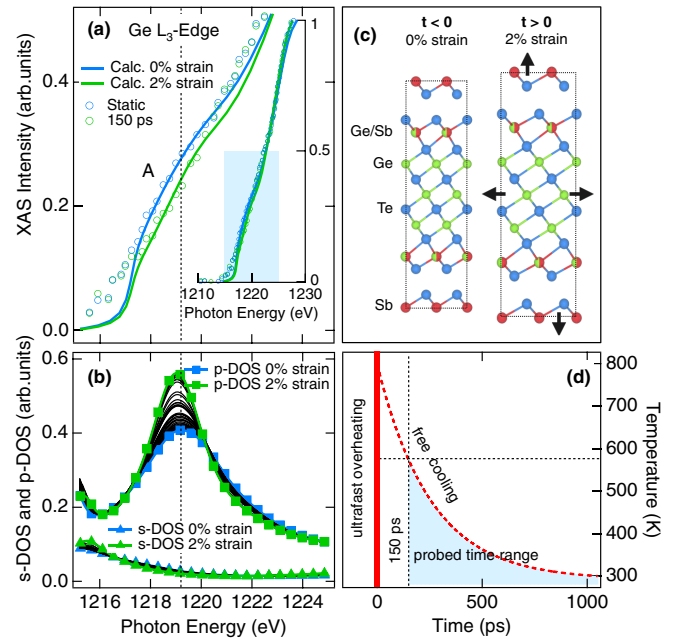
FIG. 2. Panel (a) and inset therein: the experimental (open dots) Ge L_3 thresholds measured at time delays $\delta t = 0$ (unpumped blue curves) and 150 ps (green dots) are qualitatively compared to the calculated (continuous curves) Ge L_3 thresholds. The simulated line shapes have been calculated for no expansion and 2% expansion of the lattice parameters, respectively. Panel (b) displays the Ge 3p- and 4s-DOS curves calculated for a series of strain values (0–2%) of the crystal lattice. Panel (c) sketches the CSL crystal cell before (equilibrium) and after (heated state) the arrival of the laser pulse. Therein a simplified version of the observed phenomenon is visually represented: the sudden change in temperature drives a lattice expansion of the CSL. The lattice will recover the initial state after complete thermal dissipation is achieved ($T_{in} = T_{fin}$). Panel (d) ΔT calculated through Eq. (4).

Ge L_3 edge for a series of stretched structures of a known stable structure [28] [displayed in Fig. 2(c) for positive and negative δt], where the unit cell parameters were varied by some tenth of a percent (see details in Supplemental Material [32], paragraph IV). Here the assumption, validated by the experimental observation that no phase transition occurs after the absorption of the laser pulse, is that the symmetries of the Ge sites remain unchanged after the laser illumination. The theoretical Ge L_3 XAS spectra shown in Fig. 2 are obtained by averaging the MS XAS line shape calculated for each Ge crystal site within the CSL unit cell.

In Fig. 2(a) the average Ge L_3 XAS calculated for the undistorted structure and the largest stretched structure are displayed in the close-up energy region of the A bump, and they are qualitatively compared with the equilibrium and 150 ps delayed experimental data. The inset of Fig. 2(a) displays the calculated and experimental L_3 spectra over an extended photon energy range. The calculated spectra nicely reproduce the overall experimental line-shapes, while the maximum observable change in time of A is also well reproduced for a maximum 2% lattice expansion.

TABLE II. Thermoelastic parameters of the out-of-equilibrium CSL.

	CSL (this work)	References
τ_0	255 ps	
α_L	6×10^{-5} K^{-1}	2.44×10^{-5} GST$_{225}$ [42,43]
$\delta\sigma$	2% $\frac{\Delta L}{L}$	
$\Delta T_{/pulse}$	~ 300 K	
$\frac{\Delta T}{\tau_0}$	$\sim 10^{12}$ K/s	[36, p. 261][37,38]

In Fig. 2(b), the calculated *s*- and *p*-symmetry DOSs of Ge are also reported, while *d* contributions are negligible in this energy range. The *p*-projected DOSs display a prominent feature peaked at 1219 eV [matching the photon energy range of the feature A in Fig. 1(b)], whose intensity changes as a function of lattice strain. Notably, a tiny change of the *s*-projected DOSs is also observed, which is consistent with the Ge *s-p* hybridization.

This phenomenological analysis of the experimental data suggests that the detected changes measured at the onset of the Ge L_3 absorption edge, between the sample at equilibrium and after the photoexcitations, i.e., feature A in Fig. 1(b), should originate from lattice strains. This mechanism is further supported by considering that the bonding overlap between the directional *p* orbitals of Ge and the first nearest neighbors is strongly affected even by a small lattice expansion/contraction, while the almost spherical *s* orbitals are only slightly perturbed. On a side note, this observation is also relevant in terms of the ferroelectric properties of the medium, because stretched *p* bonds can increase the local electric dipole contribution to the overall polarizability.

Henceforth, consistently with the above scenario, the crystal structure undergoes a sudden lattice expansion corresponding to a fast temperature increase due to the absorption of the ultrafast pump pulse [41]. Then, both the out-of-equilibrium electronic and phonon subsystems and the lattice relax, following the heating thermal dissipation at a cooling rate of 10^{12} K/s [Figs. 2(c) and 2(d)].

The average temperature distribution $T(t)$ in the film is calculated from Fourier's law in one dimension, assuming that the electrons and phonons in the system remain in thermal equilibrium. This changing temperature distribution creates a structural strain that can be calculated as

$$\frac{\Delta L}{L} = \delta\sigma = -\alpha_L \delta T. \qquad (3)$$

Since any assumption about the strength of the electron-electron and electron-phonon couplings is neglected, it is safe to assume thermal relaxation between the electron and phonon baths [44].

Considering a consistent thermodynamical approach, ΔT can be calculated through

$$\Delta Q = \rho V \int_{RT}^{T} c_p dT \qquad (4)$$

where ρ is the film density [45], c_p the specific heat, V the heated volume, and ΔQ the overall energy absorbed per laser pulse (Table I). This approach allows us to predict an average temperature increase $\Delta T \cong 300$ K, per pulse, of the heated volume (see Supplemental Material [32], paragraphs II and III for a detailed discussion). Consequently, α_L can be calculated for our CSL sample from Eq. (4), which results in a factor ~ 2.5 higher than the GST$_{225}$ case (both values are reported in Table II). This implies that, at least during the fast thermal quenching, the CSL structure is softer (higher α_L) then the bulk case.

Finally, it is important to underline that the extrapolated value of ΔT, for time delays below 150 ps [Fig. 2(d)], does not exceed the melting temperature of the superlattice [46]. Combining this finding with the experimental observation that no phase transformation (e.g., melting) is observed by means of tr-XAS, we demonstrate that ultrafast optical overheating is a reversible process at this laser fluence regime and photon energy.

IV. CONCLUSIONS

In conclusion, the dynamics of the Ge-Te local atomic structure in a CSL, during the free cooling phase of an ultrafast-heating–fast-cooling cycle is revealed by time resolved XAS and first-principle theory modeling.

In addition to probing the atomic local structure, our approach reveals the significant impact of the lattice strain on the strength of bonds between atoms, from which strongly depends the quenching dynamics and, for example, the melting kinetics of a solid.

Our method is used here to (i) interpret the observed XAS spectral changes in terms of a dynamical microstructural picture of the Ge $4sp$-bonding relaxation and (ii) estimate relevant elastic properties of the out-of-equilibrium state of the CSL film.

Furthermore, by combining thermoelastic considerations and a microscopic multiple scattering approach, we establish a direct connection between the structural microscopic evolution and the dielectric response in a CSL, which is fundamental for developing a microscopic theory for ultrafast phase transition and ultimately designing PCMs with improved performances.

All together these results can open the route for future studies aimed to clarify the role of a transient structural strain on the strength of bonds between atoms in phase change materials in the proximity or even during a phase transition.

[1] M. Wuttig and N. Yamada, Nat. Mater. **6**, 824 (2007).

[2] M. H. R. Lankhorst, B. W. S. M. M. Ketelaars, and R. A. M. Wolters, Nat. Mater. **4**, 347 (2005).

[3] J. Tominaga, P. Fons, A. Kolobov, T. Shima, T. C. Chong, R. Zhao, H. K. Lee, and L. Shi, Jpn. J. Appl. Phys. **47**, 5763 (2008).

[4] R. Simpson, P. Fons, A. Kolobov, T. Fukaya, M. Krbal, T. Yagi, and J. Tominaga, Nat. Nanotechnol. **6**, 501 (2011).

[5] D. A. Baker, M. A. Paesler, G. Lucovsky, S. C. Agarwal, and P. C. Taylor, Phys. Rev. Lett. **96**, 255501 (2006).

[6] X. Yu and J. Robertson, Sci. Rep. **5**, 12612 (2015).

[7] Z. Sun, J. Zhou, and R. Ahuja, Phys. Rev. Lett. **96**, 055507 (2006).

[8] W. Wełnic, S. Botti, L. Reining, and M. Wuttig, Phys. Rev. Lett. **98**, 236403 (2007).

[9] Z. Sun, J. Zhou, and R. Ahuja, Phys. Rev. Lett. **98**, 055505 (2007).

[10] A. Klein, H. Dieker, B. Späth, P. Fons, A. Kolobov, C. Steimer, and M. Wuttig, Phys. Rev. Lett. **100**, 016402 (2008).

[11] S. Caravati, M. Bernasconi, T. D. Kühne, M. Krack, and M. Parrinello, Phys. Rev. Lett. **102**, 205502 (2009).

[12] S. H. Lee and H. K. Henisch, J. Nron-Cryst. Solids **11**, 192 (1972).

[13] K. W. Böer and S. R. Ovshinsky, J. Appl. Phys. **41**, 2675 (1970).

[14] K. Makino, J. Tominaga, A. V. Kolobov, P. Fons, and M. Hase, Appl. Phys. Lett. **101**, 232101 (2012).

[15] L. Waldecker, T. A. Miller, M. Rude, R. Bertoni, and J. Osmond, Nat. Mater. **14**, 991 (2015).

[16] K. V. Mitrofanov, P. Fons, K. Makino, R. Terashima, T. Shimada, A. V. Kolobov, J. Tominaga, V. Bragaglia, A. Giussani, R. Calarco, H. Riechert, T. Sato, T. Katayama, K. Ogawa, T. Togashi, M. Yabashi, S. Wall, D. Brewe, and M. Hase, Sci. Rep. **6**, 20633 (2016).

[17] M. Le Gallo, A. Athmanathan, D. Krebs, and A. Sebastian, J. Appl. Phys. **119**, 025704 (2016).

[18] G. Bruns, P. Merkelbach, C. Schlockermann, M. Salinga, M. Wuttig, T. D. Happ, J. B. Philipp, and M. Kund, Appl. Phys. Lett. **95**, 043108 (2009).

[19] D. Krebs, S. Raoux, C. T. Rettner, G. W. Burr, M. Salinga, and M. Wuttig, Appl. Phys. Lett. **95**, 082101 (2009).

[20] K. Kohary and C. D. Wright, Appl. Phys. Lett. **98**, 223102 (2011).

[21] J. A. Vázquez Diosdado, P. Ashwin, K. I. Kohary, and C. D. Wright, Appl. Phys. Lett. **100**, 253105 (2012).

[22] L. Cao, L. Wu, W. Zhu, X. Ji, Y. Zheng, Z. Song, F. Rao, S. Song, Z. Ma, and L. Xu, Appl. Phys. Lett. **107**, 242101 (2015).

[23] X. Zhou, J. Kalikka, X. Ji, L. Wu, Z. Song, and R. E. Simpson, Adv. Mater. **28**, 3007 (2016).

[24] W. Gawelda, J. Siegel, C. N. Afonso, V. Plausinaitiene, A. Abrutis, and C. Wiemer, J. Appl. Phys. **109**, 123102 (2011).

[25] M. Krbal, A. V. Kolobov, P. Fons, J. Tominaga, S. R. Elliott, J. Hegedus, and T. Uruga, Phys. Rev. B **83**, 054203 (2011).

[26] M. Krbal, A. Kolobov, P. Fons, K. V. Mitrofanov, Y. Tamenori, J. Hegedüs, S. R. Elliott, and J. Tominaga, Appl. Phys. Lett. **102**, 111904 (2013).

[27] P. Castrucci, R. Gunnella, M. De Crescenzi, M. Sacchi, G. Dufour, and F. Rochet, Phys. Rev. B **60**, 5759 (1999).

[28] B. Casarin, A. Caretta, J. Momand, B. J. Kooi, M. A. Verheijen, V. Bragaglia, R. Calarco, M. Chukalina, X. Yu, J. Robertson, F. R. L. Lange, M. Wuttig, A. Redaelli, E. Varesi, F. Parmigiani, and M. Malvestuto, Sci. Rep. **6**, 22353 (2016).

[29] J. Momand, R. Wang, J. Boschker, M. A. Verheijen, R. Calarco, and B. J. Kooi, Nanoscale **7**, 19136 (2015).

[30] L. Stebel, M. Malvestuto, V. Capogrosso, P. Sigalotti, B. Ressel, F. Bondino, E. Magnano, G. Cautero, and F. Parmigiani, Rev. Sci. Instrum. **82**, 123109 (2011).

[31] A. Caretta, B. Casarin, P. Di Pietro, A. Perucchi, S. Lupi, V. Bragaglia, R. Calarco, F. R. L. Lange, M. Wuttig, F. Parmigiani, and M. Malvestuto, Phys. Rev. B **94**, 045319 (2016).

[32] See Supplemental Material at http://link.aps.org/supplemental/ 10.1103/PhysRevB.94.094310 for a detailed discussion and calculations.

[33] P. Fons, P. Rodenbach, K. V. Mitrofanov, A. V. Kolobov, J. Tominaga, R. Shayduk, A. Giussani, R. Calarco, M. Hanke, H. Riechert, R. E. Simpson, and M. Hase, Phys. Rev. B **90**, 094305 (2014).

[34] P. Fons, H. Osawa, A. V. Kolobov, T. Fukaya, M. Suzuki, T. Uruga, N. Kawamura, H. Tanida, and J. Tominaga, Phys. Rev. B **82**, 041203(R) (2010).

[35] http://henke.lbl.gov/optical_constants/filter2.html (accessed December 7, 2015).

[36] *Phase Change Materials: Science and Applications*, edited by S. Raoux and M. Wuttig (Springer, New York, 2010).

[37] P. Jund, D. Caprion, and R. Jullien, Phys. Rev. Lett. **79**, 91 (1997).

[38] J. Hegedüs and S. R. Elliott, Nat. Mater. **7**, 399 (2008).

[39] J. J. Rehr, J. J. Kas, M. P. Prange, A. Sorini, Y. Takimoto, and F. Vila, C. R. Phys. **10**, 548 (2009).

[40] J. J. Rehr, J. J. Kas, F. D. Vila, M. P. Prange, and K. Jorissen, Phys. Chem. Chem. Phys. **12**, 5503 (2010).

[41] C. Thomsen, H. T. Grahn, H. J. Maris, and J. Tauc, Phys. Rev. B **34**, 4129 (1986).

[42] I. M. Park, J. K. Jung, S. O. Ryu, K. J. Choi, B. G. Yu, Y. B. Park, S. M. Han, and Y. C. Joo, Thin Solid Films **517**, 848 (2008).

[43] J. Kalb, F. Spaepen, T. P. Leervad Pedersen, and M. Wuttig, J. Appl. Phys. **94**, 4908 (2003).

[44] G. L. Eesley, Phys. Rev. B **33**, 2144 (1986).

[45] J. L. Battaglia, A. Kusiak, V. Schick, A. Cappella, C. Wiemer, M. Longo, and E. Varesi, J. Appl. Phys. **107**, 044314 (2010).

[46] N. Yamada, E. Ohno, K. Nishiuchi, N. Akahira, and M. Takao, J. Appl. Phys. **69**, 2849 (1991).